

reaction of MT (3.57 mmol) and NOBF_4 (0.73 mmol) in 20 mL of acetonitrile at 25 °C afforded 0.24 mmol of biaryls and 3.24 mmol of recovered MT.

Cyclopropylbenzene (2.86 mmol) was added to a solution (0.74 mmol) of NO^+BF_4^- in 40 mL of acetonitrile at 25 °C under an argon atmosphere. The resultant yellow solution was stirred for 7 h at 25 °C in the dark, quenched with 10% NaHCO_3 , and extracted with diethyl ether to afford 5-phenylisoxazoline (0.51 mmol) by column chromatography with silica gel. $^1\text{H NMR}$ (CDCl_3): δ 2.94 (d, d, d, $J = 17.6, 8.2, 1.7$ Hz), 3.43 (d, d, d, $J = 17.6, 11, 1.7$ Hz), 5.51 (d, d, $J = 8.2, 10.9$ Hz), 7.18 (br t), 7.32 (m). $^{13}\text{C NMR}$ (CDCl_3): δ 43.7 (t, $J = 38$ Hz), 79.8 (d, $J = 29$ Hz), 125.7 (d, $J = 23$ Hz), 128.1, 128.7 (d, $J = 22$ Hz), 139.8 (s), 145.5 (d, $J = 23$ Hz). IR (neat liquid):^{40a} 3065, 3030, 2924, 2854, 1673, 1602, 1497, 1455, 1434, 1363, 1286, 1265, 1209, 1075, 1026, 920, 850, 759, 702 cm^{-1} . GC-MS, m/z (%) 147 (M^+ , 15), 146 (10), 130 (5), 116 (5), 115 (17), 105 (23), 104 (100), 91 (18), 78 (49), 77 (43), 76 (6), 69 (25), 65 (12), 63 (12), 51 (47), 50 (25), 42 (33), 41 (12). Anal. Calcd for $\text{C}_9\text{H}_9\text{NO}$: C, 73.44; H, 6.16; N, 9.52. Found: C, 72.81; H, 6.18; N, 9.29. Protonated 5-phenylisoxazoline was obtained from the mixture of NOPF_6 with cyclopropylbenzene in CD_3NO_2 . $^1\text{H NMR}$: δ 3.9 (d, d, d, $J = 21.5, 10.5, 1.96$ Hz), 4.38 (d, d, d, $J = 21.5, 10.5, 2.3$ Hz), 6.32 (t, $J = 10.5$ Hz), 7.53 (m), 8.85 (d, d, $J = 2.22, 1.95$ Hz). $^{13}\text{C NMR}$: δ 42.4, 87.6, 128.4, 130.6, 131.7, 159.0.

Appendix

The degree of charge transfer in the EDA complexes as described in eq 20 was developed from the relationship⁵⁵

$$Z = (\Delta k/k)/(1 - k'/k) \quad (36)$$

where k and k' are the force constants for NO^+Y^- and NO , respectively, and Δk is the force-constant difference between the free nitrosonium salt and that of the EDA complex (k_c). The force constants for the diatomic species are related to the N–O vibrational frequencies by the general expression $k_i = 4\pi^2c^2\mu\nu_i^2$, where c is the speed of light and μ the reduced mass.⁷⁹ If the N–O vibrational frequency (ν_c) in the EDA complex is also approximated by the diatomic molecule expression, i.e., $\nu_c = (2\pi c)^{-1} \cdot (k_c/\mu)^{1/2}$, then $\Delta k \approx 4\pi^2c^2\mu(\nu_{\text{NO}}^{+2} - \nu_c^2)$. Substitution into eq 36 yields eq 20.

The relationship between the ^{13}C chemical shift ($\delta(^{13}\text{C})$) and the π -electron density (ρ_i) on a carbon atom in eq 22 was obtained from the plot of known $\delta(^{13}\text{C})$ values from conjugated systems¹⁹

(79) Herzberg, G. L. *Infrared and Raman Spectra*; van Nostrand: Princeton, NJ, 1945; p 62.

against the calculated π -electron densities of the corresponding carbon atom. The latter were obtained from the simple relationship between the Hückel charge density (ρ_{av}) and the number of electrons per ring carbon atom. The ^{13}C chemical shifts used in the correlation were¹⁹ [^{13}C ppm (averaged), π -electron density] 1,2,3,4-tetramethylcyclobutadiene dication [209.7, 0.5], 1,3,5,7-tetramethylcyclooctatetraene dication [176.7, 0.5], 1,2-dimethyl-3,4-benzocyclobutene dication [167.9, 0.75], anthracene dication [159.1, 0.857], tropylium [155.4, 0.857], benzotropenium [146.9, 0.909], benzenonium [165.02, 0.80], heptamethylbenzenonium [172.98, 0.80], biphenylene dication [160.9, 0.833], pyrene dication [156.0, 0.875], tetracene dication [150.6, 0.888], perylene dication [144.8, 0.900], octalene [132.6, 1], anthracene [128.0, 1], naphthalene [128.5, 1], benzene [129.8, 1], biphenylene [132.5, 1], 1,3-cyclohexadiene [125.45, 1], cyclohexadienyl anion [98.64, 1.2], 1,1-dimethylcyclohexadienyl anion [102.76, 1.2], fluorenyl anion [116.7, 1.08], indenyl anion [113.5, 1.111], anthracene dianion [115.1, 1.143], benzocycloheptatrienyl dianion [103.7; 1.167], octalene dianion [111.9, 1.143], octalene tetraanion [88.0, 1.286]. From the correlation of C^{13} chemical shift with the π -electron density at a carbon atom, the linear relationship ($r = 0.97$) in eq 22⁸⁰ was obtained. The π -electron densities of the aromatic carbon atoms in the $[\text{ArH}, \text{NO}^+]$ complexes were obtained from eq 22. The total charge (q) was taken as the sum of π -electron deficiency at each carbon atom [$\sum(1 - \rho_i)$], which was equivalent to the positive charge density on the arene ring of the $[\text{ArH}, \text{NO}^+]$ complexes.

Acknowledgment. We thank J. D. Korp for crystallographic assistance, M. Narayanan (Shell Development) for the ^{13}C CP/MAS NMR studies, T. A. Albright for a helpful discussion of structures, and the National Science Foundation, Robert A. Welch Foundation, and Texas Advanced Research Program for financial support.

Supplementary Material Available: Tables of complete bond lengths, bond angles, and atomic coordinates and the numbering scheme for [mesitylene, NOSbCl_6] (3 pages). Ordering information is given on any current masthead page.

(80) Such a relationship was originally established by Spiess and Schneider^{19a} on the basis of fewer cations. For the extensive use of the correlation, see refs 19b–p.

Excited-State and Ground-State Reactivities of Para-Substituted Benzyl Radicals toward Molecular Oxygen

Kunihiro Tokumura,* Tomomi Ozaki, Hideyo Nosaka, Yoko Saigusa (Ejiri), and Michiya Itoh

Contribution from the Faculty of Pharmaceutical Sciences and the Division of Life Sciences, Graduate School, Kanazawa University, Takara-machi, Kanazawa 920, Japan.

Received June 21, 1990. Revised Manuscript Received February 19, 1991

Abstract: The quenching rates of the 1A_2 fluorescence-state p -X-benzyls ($X = \text{F}, \text{Cl}, \text{OCH}_3$, and OCH_2ph) by molecular oxygen were determined to be $(1.8\text{--}2.3) \times 10^{10} \text{ M}^{-1} \text{ s}^{-1}$, which are about 1 order of magnitude higher than the ground-state oxygenation rates. Physical quenching at the diffusion-limited rate and oxygenation reaction at a lower rate were demonstrated for the reactivities of the excited state (1A_2) and the ground state (1B_2) toward molecular oxygen, respectively. A poor quenching rate of $6.7 \times 10^9 \text{ M}^{-1} \text{ s}^{-1}$ for p -cyanobenzyl in the 2B_2 fluorescent state implies that the excited-state oxygenation competes with the physical quenching. The oxygenation rate of benzyl radical in the ground state (1B_2) was reduced by the introduction of stabilizing substituents (Cl, phenyl, Br, NO_2 , and CN) at the para position. A good correlation was found between the oxygenation rate and the free radical substituent parameter (σ^*) based upon the NBS bromination of 4-substituted 3-cyanotoluene.

The oxygenation of benzyl radical to form benzylperoxy radical has been studied¹⁻⁵ previously in order to elucidate the primary

process of liquid-phase autoxidation and gas-phase photochemical smog. By monitoring the decay of the transient $\text{D}_n \leftarrow \text{D}_0$ ab-

sorption of benzyl radical in the presence of various concentrations of oxygen, the respective oxygenation rate constants have been determined to be $(2-4) \times 10^9 \text{ M}^{-1} \text{ s}^{-1}$,^{2,3} in liquid solvents with low viscosity and $(6-9) \times 10^8 \text{ M}^{-1} \text{ s}^{-1}$ $((0.99-1.5) \times 10^{-12} \text{ cm}^3 \text{ molecule}^{-1} \text{ s}^{-1})$ ^{4,5} in the vapor phase at room temperature.

Relatively long lived doublet-doublet fluorescence of various para-substituted benzyl radicals (*p*-X-benzyl) has been confirmed by the recent tandem laser pulse excitation of halide precursors in hexane at room temperature.⁶⁻⁹ Such long fluorescence lifetimes enable us to examine the excited-state reactivity, and thus it seems worthwhile to compare this with the ground-state oxygenation reactivity.

During this work, we found a remarkable para-substituent effect upon the oxygenation of benzyl radical in the ground state ($1B_2$). Upon the $D_1 \leftarrow D_0$ excitation of the *p*-X-benzyl radicals (X = F, Cl, OCH₃, OCH₂ph, and CN), about 1 order of enhancement was confirmed for the rate constants of the reaction between *p*-X-benzyl and molecular oxygen. A notably poor quenching rate was obtained for *p*-cyanobenzyl in the excited state ($2B_2$). The effects of the electronic excitation and para substitution are discussed.

Experimental Section

Benzyl chloride (Nakarai), 4-(chloromethyl)anisole (Tokyo Kasei), 4-fluorobenzyl chloride (Aldrich), 4-chlorobenzyl chloride (Nakarai), α -chloro-*p*-xylene (Nakarai), and 1-(chloromethyl)naphthalene (Nakarai) were used after distillation under reduced pressure. α -Bromo-*p*-tolunitrile (Aldrich), α -bromo-*m*-tolunitrile (Aldrich), 4-bromobenzyl bromide (Aldrich), 4-(chloromethyl)biphenyl (Aldrich), 4-nitrobenzyl chloride (Nakarai), and 4-(benzyloxy)benzyl chloride (Aldrich) were used after recrystallization from ethanol. Spectral grade hexane (Nakarai) was used as solvent. Just prior to the experiment, a mixture of oxygen and nitrogen gas of known composition was passed through a hexane solution containing benzyl halide or naphthyl halide for 10 min. The concentration of dissolved oxygen in hexane at 298 K was calculated on the basis of the reported solubility of $3.09 \times 10^{-3} \text{ M}$ under atmospheric air containing 20.946 vol % oxygen.¹⁰

Transient absorption and fluorescence spectra were measured by a laser flash apparatus with and without the monitoring pulsed xenon flash, respectively. The 248-nm pulse (14-ns fwhm and 75-mJ energy) from an excimer laser (Lambda Physik EMG 50E) was employed to induce the fragmentation of halomethyl compounds, yielding a benzylic radical and a halogen atom. In order to selectively excite the ground-state radical, a 308-nm pulse of an excimer laser (Lambda Physik EMG 53MSC) and a 337-nm pulse of a N₂ laser (Moletron UV12) were employed. The respective second pulses induce the $D_1 \rightarrow D_0$ fluorescence of benzyl and naphthylmethyl radicals. The timing sequence of the laser pulses (248 nm followed by either 308 or 337 nm) and the monitoring xenon flash were controlled by a combination of a homemade pulse generator and a digital delay generator (Berkeley Nucleonics Corp. 7010).

Results and Discussion

$D_n \leftarrow D_0$ Absorption Spectra of Various para-Substituted Benzyl Radicals in Aerated Solution at Room Temperature. It has been predicted¹¹ that the benzyl radical with C_{2v} symmetry exhibits a significant oscillator strength in the transitions from the $1B_2$ (ground state) to higher A_2 and B_2 states, compared to the small

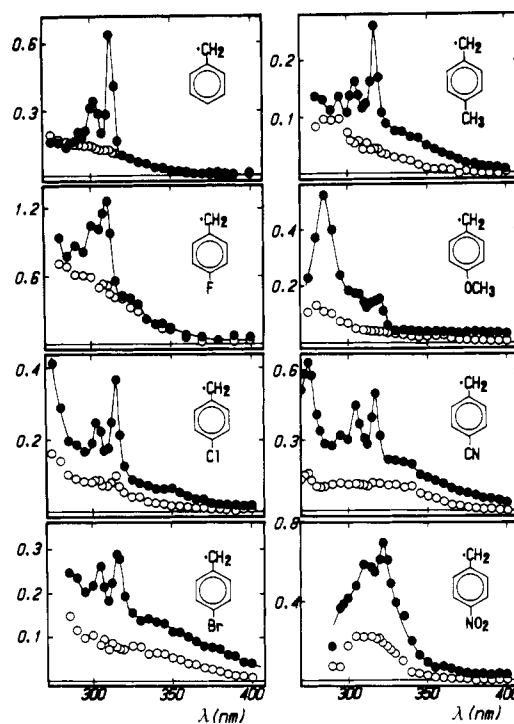


Figure 1. Transient absorption spectra (●) detected immediately after the 248-nm KrF laser photolysis of various *p*-X-benzyl halides in air-saturated hexane at room temperature. Also shown are the spectra (○) detected at submicro- to microsecond ranges after laser pulse excitation. The respective delay times from the laser pulse excitation are 810 (benzyl), 3660 (*p*-fluorobenzyl), 350 (*p*-chlorobenzyl), 1290 (*p*-bromobenzyl), 1150 (*p*-methylbenzyl), 1600 (*p*-methoxybenzyl), 960 (*p*-cyanobenzyl), and 1120 ns (*p*-nitrobenzyl). A fresh solution of *p*-X-benzyl with an optical density of ca. 1 at 248 nm was used for each laser shot.

oscillator strengths (~ 0.001) exhibited for the close-lying, lowest excited doublet states ($1A_2$ and $2B_2$). The characteristic UV absorption spectrum consisting of three peaks around 310 nm has been ascribed to the $2A_2 \leftarrow 1B_2$ transition.^{12,13} Then, it has been easily detected by steady-state photolysis of toluene^{14,15} and benzyl chloride¹⁶ in rigid glass at 77 K. Furthermore, it has been detected by transient absorption spectroscopy in the pulse radiolysis of an aqueous solution of benzyl chloride at room temperature¹⁷ as well as in the laser photolysis of benzyl chloride in an oxygen-free solution at room temperature.^{6,18} On the other hand, Huggenberger and Fischer¹⁹ have reported the UV-visible $D_n \leftarrow D_0$ absorption spectra of the benzyl radical formed in the modulated photolysis of dibenzyl ketone in cyclohexane at room temperature. Signal amplification by a phase-sensitive detector allows one to employ a light source with low intensity. By applying this technique to symmetrically substituted dibenzyl ketones in cyclohexane at room temperature, the UV-visible $D_n \leftarrow D_0$ absorption spectra of some substituted benzyl radicals have been reported.²⁰

In this work, the time-resolved absorption spectra were measured by the 248-nm KrF laser pulse excitation of benzyl chloride and seven para-substituted benzyl halides in aerated hexane at room temperature, as summarized in Figure 1. All the UV absorption spectra immediately after the photolysis of *p*-X-benzyl halides (X = H, CH₃, OCH₃, CN, NO₂, Br, Cl, and F) exhibit the structured band characteristic of the $2A_2(D_n) \leftarrow 1B_2(D_0)$

(1) Zimina, G. M.; Kovacs, L. P.; Putirskaya, G. V. *Radiochem. Radioanal. Lett.* **1980**, *44*, 413.

(2) Maillard, B.; Ingold, K. U.; Scaiano, J. C. *J. Am. Chem. Soc.* **1983**, *105*, 5095.

(3) Tokumura, K.; Nosaka, H.; Ozaki, T. *Chem. Phys. Lett.* **1990**, *169*, 321.

(4) Ebata, T.; Obi, K.; Tanaka, I. *Chem. Phys. Lett.* **1981**, *77*, 480.

(5) Nelson, H. H.; McDonald, J. R. *J. Phys. Chem.* **1982**, *86*, 1242.

(6) Tokumura, K.; Udagawa, M.; Ozaki, T.; Itoh, M. *Chem. Phys. Lett.* **1987**, *141*, 558.

(7) Tokumura, K.; Ozaki, T.; Udagawa, M.; Itoh, M. *J. Phys. Chem.* **1989**, *93*, 161.

(8) Tokumura, K.; Ozaki, T.; Itoh, M. *J. Am. Chem. Soc.* **1989**, *111*, 5999.

(9) Tokumura, K.; Itoh, M. *Nippon Kagaku Kaishi* **1989**, 1311.

(10) Murov, S. L. *Handbook of photochemistry*; Marcel Dekker: New York, 1973; p 89.

(11) Foster, S. C.; Miller, T. A. *J. Phys. Chem.* **1989**, *93*, 5986 and references therein.

(12) Porter, G.; Savadatti, M. I. *Spectrochim. Acta* **1966**, *22*, 803.

(13) Hiratsuka, H.; Okamura, T.; Tanaka, I.; Tanizaki, Y. *J. Phys. Chem.* **1980**, *84*, 285.

(14) Norman, I.; Porter, G. *Proc. R. Soc. London, A* **1955**, *230*, 399.

(15) Porter, G.; Strachan, E. *Spectrochim. Acta* **1958**, *12*, 299.

(16) Shida, T. *Electronic Absorption Spectra of Radical Ions*; Elsevier: Amsterdam, 1988; p 379.

(17) Mittal, J. P.; Hayon, E. *Nature (London), Phys. Sci.* **1972**, *240*, 21.

(18) Meisel, D.; Das, P. K.; Hug, G. L.; Bhattacharyya, K.; Fessenden, R. W. *J. Am. Chem. Soc.* **1986**, *108*, 4706.

(19) Huggenberger, C.; Fischer, H. *Helv. Chim. Acta* **1981**, *64*, 338.

(20) Claridge, R. F. C.; Fischer, H. *J. Phys. Chem.* **1983**, *87*, 1960.

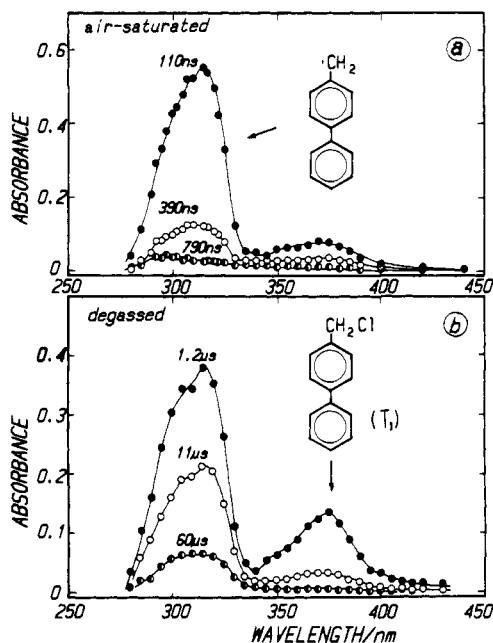


Figure 2. Time-resolved absorption spectra obtained upon the KrF laser photolysis of 4-(chloromethyl)biphenyl (0.14 mM) in air-saturated (a) and degassed (b) hexane at room temperature. Delay times from the laser pulse excitation are given beside the spectra.

absorption spectrum of the benzyl radical with C_{2v} symmetry. Those of some p -X-benzyl halides ($X = \text{CH}_3, \text{Cl}, \text{OCH}_3,$ and CN) are very similar to the published absorption spectra for p -methylbenzyl,²⁰ p -chlorobenzyl,²⁰ p -methoxybenzyl,²⁰ and p -cyanobenzyl,²¹ respectively, in oxygen-free cyclohexane at room temperature. In analogy with the $D_n \leftarrow D_0$ absorption of benzyl radical, therefore, they are ascribed to the $2A_2 \leftarrow 1B_2$ absorption spectra of the p -X-benzyl radicals. The 0,0 band of the $2A_2 \leftarrow 1B_2$ absorption is located around 317 nm for most of para-substituted benzyl radicals. Those of p -fluorobenzyl and p -nitrobenzyl are located at 310 and 323 nm, respectively, whereas a considerable substituent effect was observed for the shorter wavelength and ascribable to the intense $4B_2 \leftarrow 1B_2$ absorption of the benzyl system. As seen in Figure 1, the $4B_2 \leftarrow 1B_2$ absorption spectrum ($\lambda_{\text{max}} = 285 \text{ nm}$) of p -methoxybenzyl exhibits a considerable red shift compared to that ($\lambda_{\text{max}} = 258 \text{ nm}$)^{19,20} of benzyl radical and p -cyanobenzyl radical exhibits a slightly red-shifted $4B_2 \leftarrow 1B_2$ absorption spectrum. The intensity of the $4B_2 \leftarrow 1B_2$ absorption band cannot be directly compared with that of the $2A_2 \leftarrow 1B_2$ absorption spectrum, because no correction was made for the absorption bleaching of benzyl halide.

Figure 2 shows the time-resolved absorption spectra obtained by the 248-nm laser photolysis of 4-(chloromethyl)biphenyl in air-saturated and degassed hexane at room temperature. Both UV and visible absorption bands ($\lambda_{\text{max}} = 315$ and 375 nm) decay faster in aerated solution than in degassed solution. Thus, it is implied that oxygen-sensitive transient species are responsible for those bands. The UV band is very similar to the reported $D_n \leftarrow D_0$ absorption spectrum of biphenylmethyl radical in cyclohexane at room temperature,²² while the visible band resembles the published $T_n \leftarrow T_1$ absorption spectrum of biphenyl in hexane at 300 K.²³ Thus, it is reasonable that the oxygen-sensitive UV and visible absorption bands are assigned to the $D_n \leftarrow D_0$ absorption spectrum of biphenylmethyl radical and the $T_n \leftarrow T_1$ absorption spectrum of 4-(chloromethyl)biphenyl, respectively. It is evident for the degassed system that the second-order decay of the UV $D_n \leftarrow D_0$ absorption is slower than the decay of the visible $T_n \leftarrow$

T_1 absorption. In the air-saturated system, on the other hand, the UV $D_n \leftarrow D_0$ absorption decays faster than the visible $T_n \leftarrow T_1$ absorption. These facts indicate that the oxygenation of biphenylmethyl radical is more effective than the triplet quenching by oxygen.

It is considered that a heavy bromine or a chlorine atom directly attached to the benzene ring in p -X-benzyl halides ($X = \text{Br}$ or Cl) enhances the $S \rightarrow T$ intersystem crossing. The broad band ($\lambda_{\text{max}} = 350 \text{ nm}$) detected upon the 248-nm laser pulse excitation of p -bromotoluene in degassed hexane has been assigned to the $T_n \leftarrow T_1$ absorption spectrum.³ Assuming that both p -X-benzyl halides and p -X-toluenes exhibit similar $T_n \leftarrow T_1$ absorption spectra, the broad transient absorption spectra of p -X-benzyl halides may be attributable to their $T_n \leftarrow T_1$ absorption spectra. The superposition of absorption spectra due to the ground-state radical and its precursor in the lowest triplet state is thus demonstrated for the transient absorption spectra immediately after the laser photolysis of p -chlorobenzyl chloride and p -bromobenzyl bromide.

In the transient absorption spectrum of α -chloro- p -xylene immediately after the laser photolysis, a broad spectrum is also superimposed on the structured $2A_2 \leftarrow 1B_2$ absorption spectrum of p -methylbenzyl radical. However, it is unlikely to assign the broad spectrum to the $T_n \leftarrow T_1$ absorption of the p -xylene, since no heavy atom is present in it. The formation of p -xylylene biradical has been excluded by the failure to detect its emission from the photolysed rigid solution of p -xylene.²⁴ In the steady UV light illumination of p -xylene in 3-methylpentane at 77 K, Friedrich and Albrecht²⁵ have demonstrated that the fluorescent methylated benzene cation is formed together with p -methylbenzyl radical. They have reported that the absorption spectrum of the cation shows a peak at 330 nm. The ionization potential of N,N,N',N' -tetramethyl- p -phenylenediamine (TMPD) in hexane at room temperature has been reported to be 4.6²⁶ or 4.99 eV,²⁷ which is considerably lower than its gas-phase ionization potential of 6.6 eV.²⁸ Assuming the similar reduction for the gas-phase ionization potential (6.96 eV) of p -methylbenzyl radical, it is probable that the 248-nm (5 eV) laser pulse induces ionization of the radical in hexane at room temperature. It has been reported²⁹ that benzyl cation in 1,2-dichloroethane exhibits a UV absorption band with a maximum at 363 nm. It is thus reasonable to ascribe the broad absorption spectrum around 350 nm to p -methylbenzyl cation. It is recognized that the multiphoton processes favored in the high-density 248-nm laser photolysis of α -chloro- p -xylene are responsible for the considerable formation of the cation. The ionization of p -methoxybenzyl radical is indicated by the fact that the gas-phase ionization potential of p -methoxybenzyl is 0.64 eV lower than that of p -methylbenzyl.³⁰ However, no significant broad spectrum of p -methoxybenzyl cation was observed,³¹ as shown in Figure 1. No appreciable absorption band is superimposed on the structured $2A_2 \leftarrow 1B_2$ absorption spectra of benzyl, p -fluorobenzyl, and p -nitrobenzyl radicals.

Determination of Rate Constants for the Oxygenation Reaction of Various Benzyl Radicals in Hexane at Room Temperature. In the oxygen-free solution, benzyl radical is subjected to a coupling reaction to form bibenzyl derivatives. The self-termination rate ($2k_t$) of benzyl radical has been reported to be $7 \times 10^9 \text{ M}^{-1} \text{ s}^{-1}$ with use of CIDNP-detected laser flash photolysis of benzyl ketones in benzene at room temperature.³² The $2k_t$ value has been

(24) Migirdicyan, E.; Baudet, J. *J. Am. Chem. Soc.* **1975**, *97*, 7400.

(25) Friedrich, D. M.; Albrecht, A. C. *Chem. Phys.* **1974**, *6*, 366.

(26) Wu, K.-C.; Lipsky, S. *J. Chem. Phys.* **1977**, *66*, 5614.

(27) Holroyd, R. A.; Russell, R. L. *J. Phys. Chem.* **1974**, *78*, 2128.

(28) Bernas, A.; Gauthier, M.; Grand, D. *J. Phys. Chem.* **1972**, *76*, 2236.

(29) Dorfman, L. M.; Sujdak, R. J.; Bockrath, B. *Acc. Chem. Res.* **1976**, *9*, 352.

(30) Harrison, A. G.; Kebarle, P.; Lossing, F. P. *J. Am. Chem. Soc.* **1961**, *83*, 777.

(31) Because of considerable red shift of the intense $4B_2 \leftarrow 1B_2$ absorption band upon the introduction of a methoxy group at the para position of benzyl, the absorptivity of p -methoxybenzyl is not significant at 248 nm. This might be the reason why the substantial absorption of p -methoxybenzyl cation is not detected in the transient absorption spectrum of p -(chloromethyl)anisole, immediately after the 248-nm KrF laser photolysis.

(21) Neta, P.; Behar, D. *J. Am. Chem. Soc.* **1981**, *103*, 103.

(22) Weir, D.; Johnston, L. J.; Scaiano, J. C. *J. Phys. Chem.* **1988**, *92*, 1742.

(23) Heinzelmann, W.; Labhart, H. *Chem. Phys. Lett.* **1969**, *4*, 20.

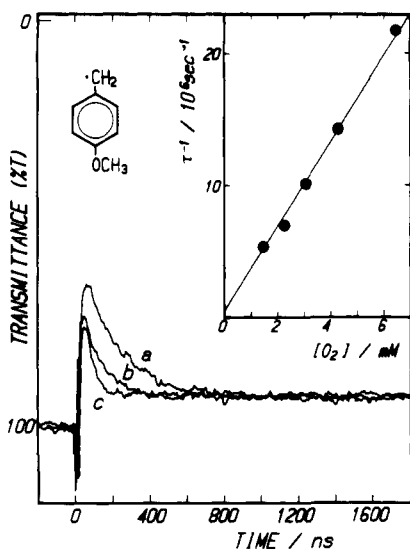


Figure 3. Exponential decay signals (a, b, and c) of the 320-nm transient $D_n \leftarrow D_0$ absorption of *p*-methoxybenzyl radical observed upon the KrF laser pulse excitation of *p*-(chloromethyl)anisole in hexane containing dissolved oxygen (1.43, 3.09, and 6.42 mM). Inset shows the plot of reciprocal lifetime of the transient absorption versus concentration of molecular oxygen.

determined to be $4.6 \times 10^9 \text{ M}^{-1} \text{ s}^{-1}$ by using the modulated photolysis of dibenzyl ketone in cyclohexane at room temperature.²⁰ The rate equation for the disappearance of radical (R^*) is expressed by eq 1. Pseudo-first-order reactions such as the

$$-d[R^*]/dt = k_1[R^*] + 2k_r[R^*]^2 \quad (1)$$

H abstraction of radical from solvent may be responsible for the first term. The rate equation in the presence of dissolved oxygen is expressed by two terms that are linear and quadratic with respect to $[R^*]$. Here, the second-order rate constant of the oxygenation

$$-d[R^*]/dt = (k_1 + k_{ox}[O_2])[R^*] + 2k_r[R^*]^2 \quad (2)$$

reaction is designated as k_{ox} . In order to evaluate the k_{ox} value, therefore, the decay of the $D_n \leftarrow D_0$ absorption should be monitored in the presence of various concentrations of oxygen. The $D_n \leftarrow D_0$ absorption of *p*-X-benzyl radical (X = H, F, OCH₃, or NO₂), without the overlapping of considerable transient absorption of other transient species such as triplet-state precursor etc. is favorable for this sort of evaluation.

The transient absorbance ($D(t) - D_\infty$) of benzyl chloride exhibits a single exponential decay. From the linear relationship between the exponential decay rate and the concentration of oxygen, the k_{ox} value for the oxygenation of benzyl radical was determined to be $2.6 \times 10^9 \text{ M}^{-1} \text{ s}^{-1}$. This is slightly less than the reported value of $2.8 \times 10^9 \text{ M}^{-1} \text{ s}^{-1}$.² By the same manner, the k_{ox} values of *p*-fluorobenzyl and *p*-nitrobenzyl were determined to be 2.9×10^9 and $8.9 \times 10^8 \text{ M}^{-1} \text{ s}^{-1}$, respectively.

Upon the KrF laser pulse excitation of *p*-(chloromethyl)anisole (CMA) in hexane containing dissolved oxygen, the 320-nm transient absorption signals due to the $D_n(2A_2) \leftarrow D_0(1B_2)$ absorption of *p*-methoxybenzyl were observed as shown in Figure 3. All the signals exhibit a single exponential decay, indicating that the oxygenation precedes the bimolecular coupling reaction. After the exponential decay, there persists a significant absorbance (D_∞) ascribable to (*p*-methoxybenzyl)peroxy radical as well as an unidentified long-lived species. The lifetime of the $D_n \leftarrow D_0$ absorption was determined from the slope of the logarithmic plot of $D(t) - D_\infty$. The reciprocal lifetimes were then plotted against the concentration of oxygen, as shown in the inset of Figure 3. From the slope of this plot, the rate constant for the oxygenation of *p*-methoxybenzyl was determined to be $3.1 \times 10^9 \text{ M}^{-1} \text{ s}^{-1}$. The same k_{ox} value has been obtained by monitoring the 280-nm D_n

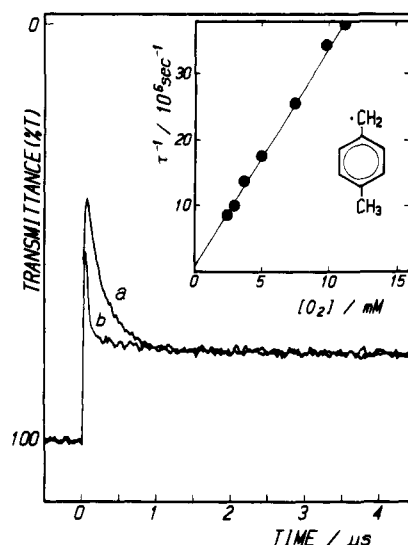


Figure 4. Decay signals (a and b) of the 315-nm transient absorption observed upon the KrF laser pulse excitation of α -chloro-*p*-xylene in hexane containing dissolved oxygen (1.64 and 9.83 mM). The reciprocal of the short-lived $D_n \leftarrow D_0$ absorption lifetime of *p*-methylbenzyl radical is plotted against the concentration of molecular oxygen and is shown in the inset.

$\leftarrow D_0$ absorption decay in the presence of various concentrations of oxygen.³ The 280-nm absorption band, uncorrected for the depletion of CMA, can be ascribed to very intense $4B_2 \leftarrow 1B_2$ absorption of *p*-methoxybenzyl radical. It is therefore reasonable to neglect that the additional absorption due to possible *p*-methoxybenzyl cation and CMA triplet is neglected at 280 nm. These arguments indicate that the additional absorption contribution is negligible even at 320 nm.

As has been described previously, the $D_n(2A_2) \leftarrow D_0(1B_2)$ absorption spectrum of *p*-methylbenzyl radical is accompanied by the absorption of *p*-methylbenzyl cation. Upon the 248-nm laser pulse excitation of α -chloro-*p*-xylene in hexane containing dissolved oxygen (1.64 and 9.83 mM), 315-nm transient absorption signals were detected in the microsecond time domain, as shown in Figure 4. Taking the invariant absorbance over the 100- μ s time domain following the initial decay as D_∞ , a double exponential fit was made for the transient absorbance ($D(t) - D_\infty$). The lifetimes of the $D_n \leftarrow D_0$ absorption in the presence of various concentrations of oxygen were determined together with the lifetime (ca. 750 ns) of the long-lived component. The plot of the reciprocal lifetime against oxygen concentration gave a straight line, as shown in the inset of Figure 4. From the slope of this straight line, the oxygenation rate of *p*-methylbenzyl radical was evaluated to be $3.4 \times 10^9 \text{ M}^{-1} \text{ s}^{-1}$.

The transient absorption observed upon the 248-nm laser photolysis of *p*-bromobenzyl bromide (BBB) in the presence of oxygen does not exhibit a single exponential decay, as shown in Figure 5. The inset shows the time-resolved absorption spectra for the aerated solution. The short-lived spectrum ($\lambda_{max} = 315 \text{ nm}$) is accompanied by the longer lived absorption ascribable to the $T_n \leftarrow T_1$ absorption of BBB. This implies that the triplet quenching by oxygen is less effective than the oxygenation of radical in spite of the encounter-limited nature for both of them. The spin statistical factor of $1/3$ for the oxygenation of free radical is considerably larger than that of $1/9$ for the triplet quenching by oxygen.³³ In the presence of considerable concentrations of oxygen, therefore, the lifetimes of the $D_n \leftarrow D_0$ absorption were determined by double exponential fit for the transient absorbance ($D(t) - D_\infty$). The rate constant for the oxygenation of *p*-

(32) Läufer, M.; Dreeskamp, H. *J. Magn. Reson.* **1984**, *60*, 357.

(33) Since a doublet and a triplet add up to a doublet or a quartet, the spin statistical factor of $1/3$ should be considered for the peroxy radical (doublet) formed in the oxygenation reaction, whereas a pair of triplets add up a quintet, a triplet, or a singlet. The spin statistical factor is $1/9$ for the ground state (S_0) formed during triplet quenching by molecular oxygen.

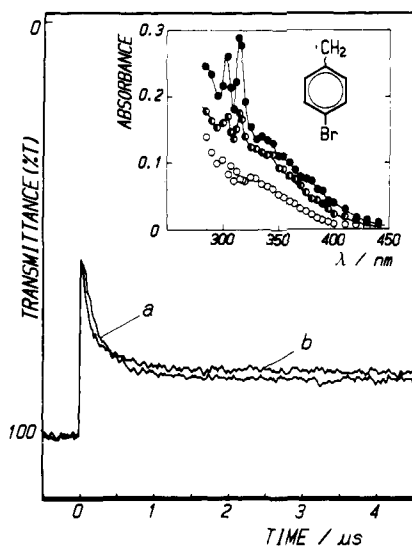


Figure 5. Decay signals (a and b) of the 315-nm transient absorption observed upon the KrF laser pulse excitation of *p*-bromobenzyl bromide in hexane containing dissolved oxygen (3.09 and 11.1 mM). Inset shows the time-resolved absorption spectra at 40 ns (O), 200 ns (Φ), and 1290 ns (●) after the laser pulse excitation.

Table I. Oxygenation Rate Constants (k_{ox}) and Radical Substituent Parameters (σ_a^* and σ^*) of Various Benzyl Radicals in Hexane at Room Temperature

free radical	σ_a^*	σ^*	k_{ox} ($M^{-1} s^{-1}$)
benzyl	0	0	2.6×10^9
<i>p</i> -fluorobenzyl	-0.011	-0.25	2.9×10^9
<i>p</i> -methoxybenzyl	0.018	-0.12	3.1×10^9
<i>m</i> -cyanobenzyl	-0.026	-0.10	3.2×10^9
<i>p</i> -methylbenzyl	0.015	-0.02	3.4×10^9
<i>p</i> -chlorobenzyl	0.011	0.08	2.0×10^9
<i>p</i> -phenylbenzyl		0.12	1.7×10^9
<i>p</i> -bromobenzyl		0.17	1.3×10^9
<i>p</i> -nitrobenzyl		0.27	8.9×10^8
<i>p</i> -cyanobenzyl	0.040	0.34	5.8×10^8

bromobenzyl radical was determined to be $1.3 \times 10^9 M^{-1} s^{-1}$. The oxygenation rates of *p*-X-benzyls (X = Cl, CN, and ph) and *m*-cyanobenzyl were determined within $\pm 20\%$ error in a similar manner. Table I lists the rate constants for the oxygenation of benzyl and various substituted benzyl radicals.

Quenching of Doublet-Doublet Fluorescence of Various Benzyl Radicals by Molecular Oxygen in Hexane at Room Temperature. Benzyl and para-substituted benzyl radicals in the ground state exhibit relatively intense $D_n \leftarrow D_0$ absorption spectra in the 290–350-nm region, as shown in Figures 1 and 2. A 308-nm XeCl laser pulse is adequate for the selective excitation of benzyl radical without excitation of benzyl halide. Higher doublet excited states (D_n) reached upon the 308-nm pulse excitation rapidly relax to the fluorescent state (D_1) via the $D_n \rightarrow D_1$ internal conversion. The red $D_1 \rightarrow D_0$ fluorescence of biphenylmethyl (*p*-phenylbenzyl) radical²² and the green ones of other benzyl radicals were easily detected by the stepwise excitation of two intense excimer laser pulses (248 and 308 nm). The fluorescence lifetimes of $< 1, 6, 2, 12,$ and 14^6 ns were determined by the computer-simulated convolution of the fluorescence signals of benzyl, *p*-bromobenzyl, *p*-phenylbenzyl, and *p*-methylbenzyl, respectively, in oxygen-free hexane at room temperature. A fluorescence lifetime of 35 ns was determined for the weak fluorescence signals of *p*-nitrobenzyl. Contrary to the short-lived and/or weak fluorescence signals, the intense fluorescence of *p*-fluorobenzyl, *p*-methoxybenzyl, *p*-chlorobenzyl, *p*-cyanobenzyl, and *p*-benzyloxybenzyl exhibit a slow exponential decay of 200,⁹ 120,⁷ 81,⁶ 58,⁸ and 58 ns, respectively. Such long-lived and intense fluorescence enabled us to study their quenching by molecular oxygen.

Figure 6 shows the oscillogram traces of the 500-nm fluorescence of *p*-cyanobenzyl in the absence and in the presence of

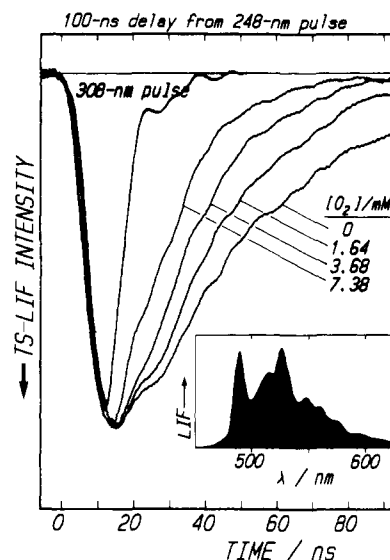


Figure 6. Two-step laser-induced fluorescence (TS LIF) signals detected upon the 308-nm pulse excitation of *p*-cyanobenzyl radical formed in the 248-nm pulse excitation of α -bromo-*p*-tolunitrile in hexane containing various concentrations of dissolved molecular oxygen. Inset shows the TS LIF spectrum assigned to the fluorescence spectrum of *p*-cyanobenzyl radical.

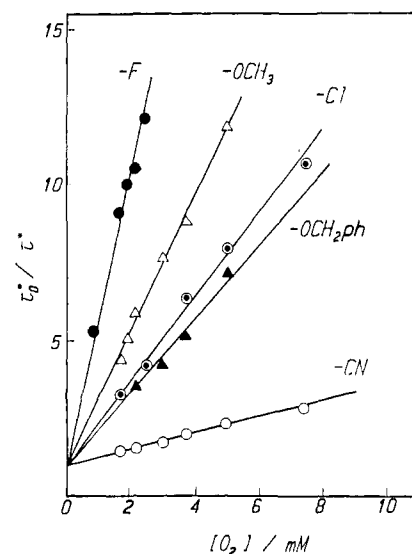


Figure 7. Stern-Volmer plots for the fluorescence lifetime of various para-substituted benzyl (*p*-X-benzyl) radicals versus concentration of molecular oxygen. X = cyano (O), benzyloxy (▲), chloro (⊙), methoxy (Δ), and fluoro (●).

dissolved oxygen. All the fluorescence signals exhibiting a single exponential decay were analyzed by convolution analysis, taking into account the shape of the 308-nm probe pulse. Taking τ_0^* as the fluorescence lifetime in oxygen-free hexane, the τ_0^*/τ^* values were plotted against the oxygen concentration (Figure 7). Each Stern-Volmer plot for the oxygen quenching of the five para-substituted benzyl radicals reveals a straight line, the slope of which represents the quenching constant. The quenching rate constants (k_{ox}^* values) were then calculated from the ratio of slope/ τ_0^* . On the other hand, the somewhat short lived (34 ns)^{34,35} $D_1 \rightarrow D_0$ fluorescence of 1-naphthylmethyl radical was detected in the KrF laser photolysis of 1-(chloromethyl)naphthalene followed by a 337-nm N_2 laser pulse excitation. The fluorescence lifetimes in the presence of various concentrations of oxygen were also determined by a computer-simulated convolution. The k_{ox}^*

(34) Tokumura, K.; Udagawa, M.; Itoh, M. *J. Phys. Chem.* **1985**, *89*, 5147.

(35) Johnston, L. J.; Scaiano, J. C. *J. Am. Chem. Soc.* **1985**, *107*, 6368.

Table II. Rate Constants (k_{ox}^* and k_{ox}) for the Fluorescence Quenching and the Ground-State Oxygenation Reaction of Various Benzylic Radicals in Solution at Room Temperature

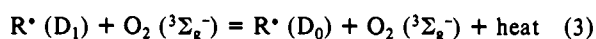
free radical	solvent	D_1	k_{ox}^* ($\text{M}^{-1} \text{s}^{-1}$)	k_{ox} ($\text{M}^{-1} \text{s}^{-1}$)	
<i>p</i> -fluorobenzyl	<i>n</i> -hexane	$1A_2$	1.9×10^{10}	2.9×10^9	<i>a</i>
<i>p</i> -chlorobenzyl	<i>n</i> -hexane	$1A_2$	1.8×10^{10}	2.0×10^9	<i>a</i>
<i>p</i> -benzyloxybenzyl	<i>n</i> -hexane	$1A_2$	2.3×10^{10}	3.1×10^9	<i>a</i>
<i>p</i> -methoxybenzyl	<i>n</i> -hexane	$1A_2$	2.2×10^{10}	3.1×10^9	<i>a</i>
<i>p</i> -cyanobenzyl	<i>n</i> -hexane	$2B_2$	6.7×10^9	5.8×10^8	<i>a</i>
1-naphthylmethyl	<i>n</i> -hexane		1.4×10^{10}		<i>a</i>
1-naphthylmethyl	cyclohexane		4.7×10^9	9.8×10^8	<i>b</i>
diphenylmethyl	cyclohexane	$1A_2$	8.7×10^9	6.3×10^8	<i>c</i>

^aThis work. ^bReference 35. ^cReference 36.

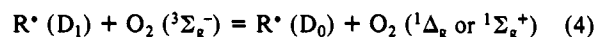
value was determined to be $1.4 \times 10^{10} \text{ M}^{-1} \text{ s}^{-1}$, which is considerably larger than that in cyclohexane ($4.7 \times 10^9 \text{ M}^{-1} \text{ s}^{-1}$)³⁵ at 298 K. The fluorescence quenching rate of diphenylmethyl radical in cyclohexane has been reported to be $8.7 \times 10^9 \text{ M}^{-1} \text{ s}^{-1}$.³⁶ Table II lists these k_{ox}^* values together with the ground-state oxygenation rate constants (k_{ox}).

Although this fluorescence quenching study cannot predict what process really takes place between the fluorescent-state benzyl and oxygen, probable quenching reactions may be argued as follows. If the oxygenation reaction takes place in the fluorescent state, analogous to that of the ground state, the fluorescence quenching rate constant should be less than the diffusion-limited rate multiplied by the spin statistical factor ($1/3$) and the steric factor. The fluorescence quenching rates of *p*-X-benzyls (X = F, Cl, OCH₃, and OCH₂ph) ranges from 1.8×10^{10} to $2.3 \times 10^{10} \text{ M}^{-1} \text{ s}^{-1}$, these being close to the diffusion-controlled rate ($2.2 \times 10^{10} \text{ M}^{-1} \text{ s}^{-1}$) calculated for hexane at 298 K. These arguments exclude the oxygenation reaction for the fluorescence quenching of such *p*-X-benzyls. The $1A_2 \leftarrow 1B_2$ excitation of *p*-X-benzyls (X = F, Cl, OCH₃, and OCH₂ph) results in about 1 order of enhancement in the rate of the reaction with molecular oxygen, (See Table II.) It is thus demonstrated that physical quenching of the excited state ($1A_2$) occurs at the diffusion-controlled rate and the oxygenation of the ground-state ($1B_2$) occurs at the lower rate.

The fluorescence quenching allowed by the spin conservation rule is expressed by eq 3. The triplet excited state ($^3\Sigma_u^+$)³⁷ with a high energy of 36096 cm^{-1} cannot be formed in the quenching of green fluorescence. On the basis of the nearly complete



recovery after the bleaching of the $D_n \leftarrow D_0$ absorption, Scaiano et al.³⁶ have claimed that no chemical reaction but the energy transfer takes place in the oxygen quenching of the fluorescent-state diphenylmethyl radical in cyclohexane at room temperature. From energetic considerations, the energy transfer from para-substituted benzyl radical (D_1) to oxygen ($^3\Sigma_g^-$) may result in the formation of singlet oxygen, as expressed by eq 4. Such an energy



transfer is analogous to the triplet-doublet (T-D) energy transfer from aromatic triplet to aromatic free radical. The T-D energy transfer has been confirmed by the detection of the sensitized doublet-doublet fluorescence of the energy acceptor, and the rate constants have been reported to be ca. $7 \times 10^9 \text{ M}^{-1} \text{ s}^{-1}$ for the energy transfer from naphthalene triplet to benzophenone ketyl in tetrahydrofuran³⁸ and $1.2 \times 10^{10} \text{ M}^{-1} \text{ s}^{-1}$ for that from *p*-methylanisole triplet to *p*-methoxybenzyl in hexane at room temperature.³⁹ Therefore, at this stage, the diffusion-controlled

physical quenching processes (eqs 3 and 4) are assumed to take place without a steric factor.

The fluorescence quenching rate ($8.7 \times 10^9 \text{ M}^{-1} \text{ s}^{-1}$) of diphenylmethyl in cyclohexane at 298 K is not so different from the diffusion-controlled rate of $7.3 \times 10^9 \text{ M}^{-1} \text{ s}^{-1}$. Taking into account that the viscosity of cyclohexane is 3 times larger than that of hexane at 298 K, our quenching rate ($1.3 \times 10^{10} \text{ M}^{-1} \text{ s}^{-1}$) for the fluorescence of 1-naphthylmethyl radical in hexane is consistent with the reported one ($4.7 \times 10^9 \text{ M}^{-1} \text{ s}^{-1}$) in cyclohexane. It should be noted that the oxygen quenching rate of 1-naphthylmethyl fluorescence is slightly less than the diffusion-controlled rate.

Substituent Effects upon Excited-State and Ground-State Reactivities of Benzyl Radicals toward Molecular Oxygen. The fluorescence quenching rate constant ($6.7 \times 10^9 \text{ M}^{-1} \text{ s}^{-1}$) of *p*-cyanobenzyl is distinctly less than the diffusion-controlled rate of ca. $2.2 \times 10^{10} \text{ M}^{-1} \text{ s}^{-1}$. This fact strongly implies that the mechanism for the quenching of the fluorescent-state *p*-cyanobenzyl is different from that of the other four para-substituted benzyl radicals. An anomalously blue-shifted $D_n \leftarrow D_1$ absorption spectrum and high H abstraction ability have been confirmed for the fluorescence-state *p*-cyanobenzyl in solution at room temperature.⁸ Furthermore, a recent three-step photoselection study⁴⁰ has demonstrated that the fluorescent state of *p*-cyanobenzyl is assigned to $2B_2$ contrary to the $1A_2$ assignment for those of benzyl, *p*-fluorobenzyl, *p*-methoxybenzyl, etc. Benzyl radical in the ground state ($1B_2$) is subjected to oxygenation. Assuming that the oxygenation of benzyl radical is favorable for B_2 states, it is probable that the oxygenation of *p*-cyanobenzyl occurs in the excited state ($2B_2$). Upon the $2B_2 \leftarrow 1B_2$ excitation of *p*-cyanobenzyl, the rate constant of the reaction with molecular oxygen was enhanced by about 1 order of magnitude. This enhancement may be attained by the occurrence of diffusion-controlled physical quenching competing with the oxygenation of the $2B_2$ state and/or by the increase in the oxygenation reactivity on going from $1B_2$ to $2B_2$. In order to elucidate this point, a quantitative analysis of the permanent depletion (an incomplete recovery) should be required for the transient absorption measurement. Unfortunately, upon excitation by a 308-nm XeCl laser pulse following the 248-nm KrF laser photolysis of α -bromo-*p*-tolunitrile, we could detect only a small depletion of the $D_n(2A_2) \leftarrow D_0(1B_2)$ absorption of *p*-cyanobenzyl.

The oxygenation of benzyl radical is virtually irreversible at room temperature.² No appreciable reverse reaction (deoxygenation of benzylperoxy radical) ensures that the observed rate constants reflect the forward oxygenation reaction exactly. It has been demonstrated that⁴¹ one might expect some kind of activation energy even for the recombination of alkyl radical. It is thus reasonable to assume that a low activation barrier exists for the oxygenation, which can be regarded as a coupling reaction between benzyl radical and oxygen biradical. It is supposed that the oxygenation rate reflects the aspects of the radical's nature such as the spin (odd electron) density at the benzylic position and/or the radical's stability through spin delocalization. Table I lists radical substituent parameters based upon the spin density^{42,43} and the radical stability^{44,45} together with the rate constants for the oxygenation of benzyl and various substituted benzyl radicals.

The ESR hyperfine coupling (hfc) constant of the benzyl radical α -hydrogen is a physical quantity related to the spin density at the benzylic position. Dust and Arnold⁴² have proposed the σ_α value defined by $1 - \text{hfc}(\alpha\text{-H}_x)/\text{hfc}(\alpha\text{-H}_0)$. Here, the α -hydrogen hfc constants of benzyl and substituted benzyl are designated as $\text{hfc}(\alpha\text{-H}_0)$ and $\text{hfc}(\alpha\text{-H}_x)$, respectively. According to them, the

(39) Tokumura, K.; Kiso, F.; Dohi, M.; Takamichi, N.; Itoh, M. *Chem. Phys. Lett.* **1989**, *163*, 509.

(40) Hiratsuka, H.; Mori, K.; Shizuka, H.; Fukushima, M.; Obi, K. *Chem. Phys. Lett.* **1989**, *157*, 35.

(41) Dannenberg, J. J.; Tanaka, K. *J. Am. Chem. Soc.* **1985**, *107*, 671.

(42) Dust, J. M.; Arnold, D. R. *J. Am. Chem. Soc.* **1983**, *105*, 1221.

(43) Wayner, D. D. M.; Arnold, D. R. *Can. J. Chem.* **1984**, *62*, 1164.

(44) Fisher, T. H.; Meierhofer, A. W. *J. Org. Chem.* **1978**, *43*, 224.

(45) Fisher, T. H.; Dershem, S. M.; Prewitt, M. L. *J. Org. Chem.* **1990**, *55*, 1040.

(36) Scaiano, J. C.; Tanner, M.; Weir, D. *J. Am. Chem. Soc.* **1985**, *107*, 4396.

(37) Herzberg, G. *Spectra of Diatomic Molecules*; Van Nostrand Reinhold: New York, 1950; pp 446-448.

(38) Hiratsuka, H.; Rajadurai, S.; Das, P. K.; Hug, G. L.; Fessenden, R. W. *Chem. Phys. Lett.* **1987**, *137*, 255.

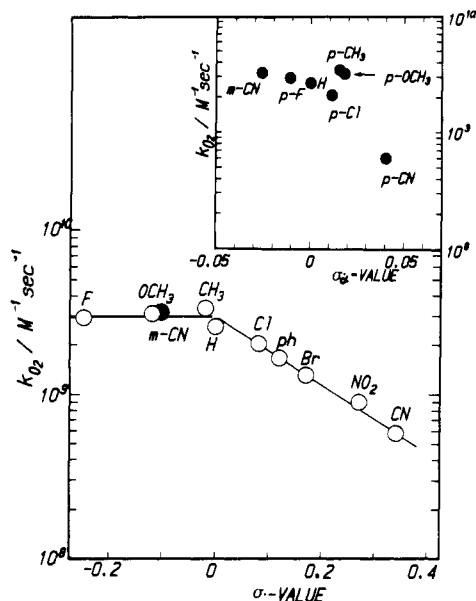


Figure 8. Oxygenation rate (k_{ox}) against the free radical substituent parameter (σ^*) based upon the NBS bromination of 4-substituted 3-cyanotoluene. Inset shows the plot of the k_{ox} value versus substituent parameter (σ_a^*), reflecting the spin density on the benzylic position.

introduction of para substituents except *p*-fluoro reduce the hfc constant, while meta substituents enhance. The respective σ_a^* values of *p*-fluorobenzyl and *m*-cyanobenzyl are -0.011 and -0.026 . Substituents that decrease the spin density at the benzylic position should have positive σ_a^* values (0.040 [*p*-CN], 0.018 [*p*-OCH₃], 0.011 [*p*-Cl], 0.015 [*p*-CH₃]). As shown in the inset of Figure 8, there is a poor correlation between the oxygenation rate constant and the σ_a^* value. The correlation factor between $\log(k_{ox}/k_{ox}^0)$ and σ_a^* was calculated to be -0.693 , which is quite unsatisfactory.

Fisher and Meierhoefer⁴⁴ have devised a σ^* value based upon the bromination of para-substituted 3-cyanotoluenes, in which the bromine atom abstracts a hydrogen from the methyl group of the toluene. They have demonstrated that the balance of the polarity of an electrophilic Br⁺ and *m*-cyano group makes the benzyl radical stabilization effect of the para substituent (X) prominent in the transition state ($[X(m-CN)C_6H_4\cdot CH_2]H^+Br^-$). It is therefore recognized that the σ^* value is a good measure of the stabilization energy of benzyl radical. The σ^* value of the *p*-methoxy group is -0.12 . Timberlake⁴⁶ has claimed that high energy orbitals (3s etc.) of the oxygen atom make the delocalization of the benzylic odd electron to the methoxy group unfavorable. On the basis that the increased spin delocalization should increase benzyl radical stability, they concluded that the methoxy substituent cannot effectively stabilize a benzyl radical and in fact seems to destabilize it.⁴⁴ It is thus recognized that the decrease in spin density at the benzylic position cannot be directly related

(46) Timberlake, J. M.; Hodges, M. L. *Tetrahedron Lett.* **1970**, *48*, 4147.

to the increase of the delocalization to substituent through the π -conjugation of the benzene ring. It has been demonstrated^{42,44} that a substantial stabilization is brought about by the substitution of an electron-withdrawing and conjugating cyano group at the para position of benzyl, while a considerable destabilization is caused by *m*-cyano and *p*-fluoro substitutions. The oxygenation rate constant ($5.8 \times 10^9 \text{ M}^{-1} \text{ s}^{-1}$) of well-stabilized *p*-cyanobenzyl is the lowest among *p*-X-benzyls, and that ($2.9 \times 10^9 \text{ M}^{-1} \text{ s}^{-1}$) of the destabilized *p*-fluorobenzyl is comparable with that ($3.2 \times 10^9 \text{ M}^{-1} \text{ s}^{-1}$) of the most destabilized *m*-cyanobenzyl.

A good correlation was obtained for the plot of oxygenation rate (k_{ox}) versus σ^* value recognized as a measure of the stabilization energy of benzyl radical. Assuming that both the energy of the transition state in the oxygenation of benzyl radical and the entropy of the activation process are little sensitive to substituent, the effect of the substituent upon the energy of benzyl radical (reactant) may be directly related to that on the oxygenation rate. Namely, the increase in activation energy due to the radical stabilization causes retardation of the oxygenation process. A straight line with a negative slope was obtained for the plot of k_{ox} vs positive σ^* , as shown in Figure 8. Five radical-stabilizing groups exhibit an excellent correlation factor of -0.989 .⁴⁷ In contrast to a good correlation between k_{ox} and positive σ^* , those at negative σ^* are approximately constant. Such a pair of straight lines in the correlation generally imply an abrupt change in the reaction mechanism. In the oxygenation of benzyl radical, however, the limitation of diffusion may be responsible for the saturation of the k_{ox} value. The spin statistical factor of $1/3$ should be considered for the reaction between a doublet (benzyl radical) and a triplet (molecular oxygen) leading to a doublet product (benzylperoxy radical). Thus, the upper limit of the k_{ox} value should be one-third of the encounter-controlled rate. Taking the diffusion-controlled rate in hexane at 298 K as $2.2 \times 10^{10} \text{ M}^{-1} \text{ s}^{-1}$ calculated from $8RT/3000\eta$, the upper limit of the oxygenation rate (k_{ox}) is $7.3 \times 10^9 \text{ M}^{-1} \text{ s}^{-1}$. It should be noted that the saturated oxygenation rate ($3.0 \times 10^9 \text{ M}^{-1} \text{ s}^{-1}$) shown in Figure 8 is considerably less than $7.3 \times 10^9 \text{ M}^{-1} \text{ s}^{-1}$. This fact strongly indicates that the steric factor is not unity for the oxygenation of benzyl radical, and the upper limit of the steric factor was estimated to be 0.41.

Conclusions

The oxygenation rate of para-substituted benzyl radical in the ground state ($1B_2$) increases with the decreasing stabilizing ability of the para substituent. However, it is limited by the diffusional encounter with the spin statistical factor ($1/3$) and the steric factor. On the other hand, physical quenching at the nearly diffusion limited rate was demonstrated for the oxygen quenching of the fluorescent state ($1A_2$). Noticeable is the alternation of the reaction mechanism from the oxygenation to the physical quenching upon the $1A_2 \leftarrow 1B_2$ excitation. Such excited-state reactivities of benzyl radical serve as an example of the photochemistry of transient species, which is significant in high-density laser photolysis.

(47) The correlation factor of -0.996 was obtained for the logarithmic plot of k_{ox}/k_{ox}^0 against σ^* value.